


# Self-error-rejecting multipartite entanglement purification for electron systems assisted by quantum-dot spins in optical microcavities

Yong-Ting Liu(刘永婷), Yi-Ming Wu(吴一鸣), and Fang-Fang Du(杜芳芳)
**Citation:**Chin. Phys. B, 2022, 31 (**5**): 050303. DOI: 10.1088/1674-1056/ac4489
Journal homepage: http://cpb.iphy.ac.cn; http://iopscience.iop.org/cpb

**What follows is a list of articles you may be interested in**

---

## Low-overhead fault-tolerant error correction scheme based on quantum stabilizer codes

Xiu-Bo Chen(陈秀波), Li-Yun Zhao(赵立云), Gang Xu(徐刚), Xing-Bo Pan(潘兴博), Si-Yi Chen(陈思怡), Zhen-Wen Cheng(程振文), and Yi-Xian Yang(杨义先)
Chin. Phys. B, 2022, 31 (**4**): 040305. DOI: 10.1088/1674-1056/ac3817

## Channel parameters-independent multi-hop nondestructive teleportation

Hua-Yang Li(李华阳), Yu-Zhen Wei(魏玉震), Yi Ding(丁祎), and Min Jiang(姜敏)
Chin. Phys. B, 2022, 31 (**2**): 020302. DOI: 10.1088/1674-1056/ac1330

## Low-loss belief propagation decoder with Tanner graph in quantum error-correction codes

Dan-Dan Yan(颜丹丹), Xing-Kui Fan(范兴奎), Zhen-Yu Chen(陈祯羽), and Hong-Yang Ma(马鸿洋)
Chin. Phys. B, 2022, 31 (**1**): 010304. DOI: 10.1088/1674-1056/ac11cf

## Improving the purity of heralded single-photon sources through spontaneous parametric down-conversion process

Jing Wang(王静), Chun-Hui Zhang(张春辉), Jing-Yang Liu(刘靖阳), Xue-Rui Qian(钱雪瑞), Jian Li(李剑), and Qin Wang(王琴)
Chin. Phys. B, 2021, 30 (**7**): 070304. DOI: 10.1088/1674-1056/abfb5c

## Quantum computation and error correction based on continuous variable cluster states

Shuhong Hao(郝树宏), Xiaowei Deng(邓晓玮), Yang Liu(刘阳), Xiaolong Su(苏晓龙), Changde Xie(谢常德), and Kunchi Peng(彭堃墀)
Chin. Phys. B, 2021, 30 (**6**): 060312. DOI: 10.1088/1674-1056/abeb0a

---

# Self-error-rejecting multipartite entanglement purification for electron systems assisted by quantum-dot spins in optical microcavities

Yong-Ting Liu(刘永婷), Yi-Ming Wu(吴一鸣), and Fang-Fang Du(杜芳芳)†

*Science and Technology on Electronic Test and Measurement Laboratory, North University of China, Taiyuan* 030051, *China*

(Received 12 October 2021; revised manuscript received 16 December 2021; accepted manuscript online 18 December 2021)

We present a self-error-rejecting multipartite entanglement purification protocol (MEPP) for $N$-electron-spin entangled states, resorting to the single-side cavity-spin-coupling system. Our MEPP has a high efficiency containing two steps. One is to obtain high-fidelity $N$-electron-spin entangled systems with error-heralded parity-check devices (PCDs) in the same parity-mode outcome of three electron-spin pairs, as well as $M$-electron-spin entangled subsystems ($2 \leq M < N$) in the different parity-mode outcomes of those. The other is to regain the $N$-electron-spin entangled systems from $M$-electron-spin entangled states utilizing entanglement link. Moreover, the quantum circuits of PCDs make our MEPP works faithfully, due to the practical photon-scattering deviations from the finite side leakage of the microcavity, and the limited coupling between a quantum dot and a cavity mode, converted into a failed detection in a heralded way.

**Keywords:** quantum communication, entanglement purification, electron-spin system

**PACS:** 03.67.–a, 03.67.Hk, 03.67.Dd, 03.65.Ud **DOI:** 10.1088/1674-1056/ac4489

## 1. Introduction

Entanglement lies at the heart of quantum mechanics and is a fundamental resource in quantum information processing (QIP), especially for accelerating quantum computation[1–3] and creating secure quantum communication, such as quantum teleportation,[4] quantum key distribution,[5–10] quantum secure direct communication,[11–19] quantum secret sharing,[4,20,21] and so on. Multipartite entangled systems[23–26] shared by the detached parties in remote locations are in a maximally entangled state for the security and the efficiency of quantum communication. However, in a practical transmission, the multipartite propagated away from each other are bound to sustain channel noises, which will inevitably degrade the entanglement or even make the maximally entangled state change into a mixed one, making quantum communication insecure. In order to establish an extensive quantum network, the quantum repeater is used to restrain the decoherence caused from the environmental noise.[27] Entanglement purification, which is one of the key constituents for quantum repeaters in the quantum communication, can distil some high-fidelity entangled quantum systems from the mixed entangled ones.[28–32]

The initial entanglement purification protocol (EPP) by Bennett *et al.*[33] and that by Deutch *et al.*[34] were presented, resorting to perfect controlled-not (CNOT) gates. Subsequently, an EPP[35] based on linear optical elements and single-photon detectors and an efficient EPP[36] with a currently obtainable parametric down-conversion (PDC) source assisted by cross-Kerr nonlinearity were introduced. EPPs have been presented in various ways, mainly consisting of conventional entanglement purification protocols (CEPPs)[33–40] and the deterministic entanglement purification protocols (DEPPs).[41,42] The latter referred to two-step DEPP based on hyerentanglement[41] and one-step DEPP based on the spatial entanglement of a pragmatic PDC source and linear optical elements.[42] Recently, much attention has been drawn to hyerentanglement purification protocols (hyper-EPPs).[43–47] For instance, Ren *et al.*[43] proposed the first two-photon hyper-EPP in the mixed polarization-spatial hyperentanglement Bell states for bit-flip errors, resorting to the nonlinear optical property of a nitrogen-vacancy center embedded in a photonic crystal cavity.

However, most of the EPPs[33–42] and hyper-EPPs[43–47] have been aimed at bipartite entangled and hyperentangled systems, respectively, and there are only few multipartite entanglement purification protocols (MEPP), including high-dimension HEPPs.[48–50] The first MEPP with CNOT gates to purify multipartite entangled systems in a Werner-type state by Murao *et al.*,[48] and then the other one to purify high-dimensional multipartite quantum systems by Cheong *et al.*[49] were proposed. Sequentially, a feasible MEPP[50] and an efficient MEPP[51] were proposed in a Greenberger–Horn–Zeilinger (GHZ) state with nondestructive quantum nondemolition detectors (QND), which were available to perform iteratively the MEPPs.

The EPP for electron-spin systems also plays a significant role in the quantum communication and quantum computation. For example, Sheng *et al.*[52] presented an MEPP

†Corresponding author. E-mail: Duff@nuc.edu.cn

© 2022 Chinese Physical Society and IOP Publishing Ltd 

for electron-spin states. The original fidelity of the MEPP was required to be lager than 0.5, meanwhile, much entangled quantum resource was discarded, leading to the relatively low efficiency. Recently, semiconducting quantum dot (QD) embedded in a optical microcavities is the best service for solid-state qubit especially in QD-spin QIP,[53] owing to the electronic spin confined in a charged QD possessing μs coherence time[54] and ps time-scale single-qubit manipulation[55,56] for controlling and measuring the spin state. Many researchers have devoted much effort to improving photon-QD-spin interactions by the integration of charged QDs amalgamated with nanophotonic micropillar cavities in experiment recently.[56–58] Besides, an entangled beam splitter,[59] a flexible two-electron-spin EPP,[60] and an optical Faraday rotation[61] can be generated with an electron-spin QD coupled to a microcavity.

In this article, we present an efficient MEPP for $N$-electron-spin systems in a GHZ state by exploiting the single-side cavity-spin-coupling system. First, we can obtain a high-fidelity $N$-electron-spin ensemble directly with fidelity-near-unity parity-check devices (PCDs), similar to the conventional MEPPs with perfect controlled-not gates.[48] Subsequently, the recycling MEPP with the entanglement link is used to reproduce some $N$-electron-spin entangled systems from subspaces. In detail, the parties in quantum communication first distil some entangled $M$-electron-spin subsystems ($2 \leq M < N$), which are discarded in the previous MEPPs,[48–50] and then they reproduce some $N$-electron-spin entangled systems with entanglement link.

## 2. Establishing an error-heralded parity-check device by QD-cavity system

As shown in Fig. 1, it is a structure diagram of the single-sided QD-cavity system. A self-organized In(Ga)As or interface-perturbation GaAs QD are placed in the wave belly of a microcavity, in which the Bragg layer at the top is all reflective and the Bragg layer at the bottom is partially reflective.[61] When the QD has an additional electron injection, a negative exciton ($X^-$) composed of two electrons and a hole can be formed optical excitation. According to Pauli exclusion principle, the electron spin state $\uparrow$ ($\downarrow$) interacts with left (right) rotationally polarized light $|L\rangle$ ($|R\rangle$), respectively. Here $\uparrow$ ($\downarrow$) represents the spin state of the extra electron, and its projection on the $z$ axis is $|+\frac{1}{2}\rangle$ ($|-\frac{1}{2}\rangle$). $|\uparrow\downarrow\Uparrow\rangle$ ($|\downarrow\uparrow\Downarrow\rangle$) represents the hole-spin state of the negative exciton ($X^-$), and its projection on the $z$ axis is $|+\frac{3}{2}\rangle$ ($|-\frac{3}{2}\rangle$). The coupled $R$-polarized ($L$-polarized) photon and the uncoupled $L$-polarized ($R$-polarized) photon get different phases and amplitudes when they are reflected by the cavity. The reflection coefficient[61–67]

$$r(\omega) = 1 - \frac{\kappa[\mathrm{i}(\omega_{X^-} - \omega) + \gamma/2]}{[\mathrm{i}(\omega_{X^-} - \omega) + \gamma/2][\mathrm{i}(\omega_{\mathrm{c}} - \omega) + \kappa/2 + \kappa_{\mathrm{s}}/2] + g^2} \tag{1}$$

can be obtained by solving the Heisenberg–Langevin equations of the motion in Eq. (2) for the cavity field operator $\hat{a}$ and negative exciton $X^-$ operator $\hat{\sigma}_-$ driven by the input field operators $\hat{a}_{\mathrm{in}}$, and combing the relation between the input field operators $\hat{a}_{\mathrm{in}}$ and the output field operators $\hat{a}_{\mathrm{out}}$ in the weak excitation approximation $\langle\hat{\sigma}_z\rangle \simeq -1$,[61–67] where the QD spin dominantly occupies the ground state

$$\begin{aligned}
\frac{\mathrm{d}\hat{a}}{\mathrm{d}t} &= -\left[\mathrm{i}(\omega_{\mathrm{c}} - \omega) + \frac{\kappa}{2} + \frac{\kappa_{\mathrm{s}}}{2}\right]\hat{a} - g\,\hat{\sigma}_- - \sqrt{\kappa}\hat{a}_{\mathrm{in}}, \\
\frac{\mathrm{d}\hat{\sigma}_-}{\mathrm{d}t} &= -\left[\mathrm{i}(\omega_{X^-} - \omega) + \frac{\gamma}{2}\right]\hat{\sigma}_- - g\hat{\sigma}_z\hat{a}, \\
\hat{a}_{\mathrm{out}} &= \hat{a}_{\mathrm{in}} + \sqrt{\kappa}\hat{a}.
\end{aligned} \tag{2}$$

Here, $\omega_{\mathrm{c}}$, $\omega_{X^-}$, and $\omega$ represent the microcavity frequency, the transition frequency of negative exciton $X^-$ and the input photon frequency, respectively. $g$ is the coupling strength between the QD and the single-sided microcavity, $\kappa$, $\kappa_{\mathrm{s}}$, and $\gamma$ are the decay rate of single-sided microcavity, leakage rate of single-sided microcavity, and decay rate of negative exciton $X^-$, respectively. In the case of coupling strength $g = 0$ (uncoupled cavity), the reflection coefficient becomes

$$r_{\mathrm{o}}(\omega) = \frac{\mathrm{i}(\omega_{\mathrm{c}} - \omega) - \kappa/2 + \kappa_{\mathrm{s}}/2}{\mathrm{i}(\omega_{\mathrm{c}} - \omega) + \kappa/2 + \kappa_{\mathrm{s}}/2}. \tag{3}$$

Therefore, the interaction between the photon and the single-sided cavity-QD system can be expressed as

$$\begin{aligned}
&|L,\uparrow\rangle \to r(\omega)|L,\uparrow\rangle, \quad |R,\uparrow\rangle \to r_{\mathrm{o}}(\omega)|R,\uparrow\rangle, \\
&|R,\downarrow\rangle \to r(\omega)|R,\downarrow\rangle, \quad |L,\downarrow\rangle \to r_{\mathrm{o}}(\omega)|L,\downarrow\rangle.
\end{aligned} \tag{4}$$

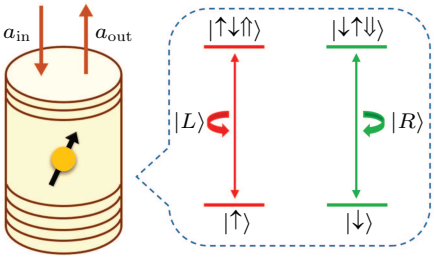



**Fig. 1.** Schematic diagram of a single-sided QD-cavity system, and the optical transitions of a QD.

We can construct a error-heralded QD block by combing the above QD-cavity system and linear optical elements, as shown in Fig. 2(a). Suppose that the single photon in the

left-polarized state $|L\rangle$ is input into the module, and the initial state of the QD spin in the single-sided cavity is $|\varphi^+\rangle = (1/\sqrt{2})(|\uparrow\rangle + |\downarrow\rangle)$. After the injected photon subsequently passes through half wave plate $H_{p1}$, QD block, $H_{p2}$, circular polarization beam splitter (CPBS), the state of the whole system evolves from $|\Phi_0\rangle = |L\rangle \otimes |\varphi^+\rangle$ to

$$|L\rangle \otimes |\varphi^+\rangle \to P|R\rangle|\varphi^-\rangle + Q|L\rangle|\varphi^+\rangle. \tag{5}$$

Here, $P$, $Q$, and $|\varphi^-\rangle$ represent $(1/2)[r_o(\omega) - r(\omega)]$, $(1/2)[r_o(\omega) + r(\omega)]$, and $(1/\sqrt{2})(|\uparrow\rangle - |\downarrow\rangle)$, respectively. Finally, the left-polarized state $|L\rangle$ reflected by the CPBS is detected by a single-photon detector (D). If the D responds, the error is detected. That is, the photon passing through the quantum block neither changes its own polarization state nor the state of the QD spin. On the contrary, if there is no response from the D, the photon passes through the quantum block, which can predict the error. Similarly, if the electron spin state is $|\varphi^-\rangle$, the final state of the system can be expressed as the following expression

$$|L\rangle \otimes |\varphi^-\rangle \to P|R\rangle|\varphi^+\rangle + Q|L\rangle|\varphi^-\rangle. \tag{6}$$

We can construct a self-error-rejecting electron-spin parity-check device (PCD) by the error-heralded QD block, as shown in Fig. 2(b). The quantum states of two-electron spins $e_1e_2$ of two QD-cavity systems can be described as

$$|\phi^\pm\rangle = \frac{1}{\sqrt{2}}(|\uparrow\uparrow\rangle \pm |\downarrow\downarrow\rangle)_{e_1e_2},$$
$$|\psi^\pm\rangle = \frac{1}{\sqrt{2}}(|\uparrow\downarrow\rangle \pm |\downarrow\uparrow\rangle)_{e_1e_2}. \tag{7}$$

We input a single photon in left-polarized state $|L\rangle$ into a quantum circuit of a error-heralded PCD. After the photon passes through VBS, the left-polarized photon $|L\rangle$ in the lower mode 1 subsequently passing through the error-heralded $QD_1$ block, $X_1$, $QD_2$ block, $X_2$, and BS, meanwhile in the upper mode 2 combining again at the BS, is detected by the detector $D_{1'}$ or $D_{2'}$.

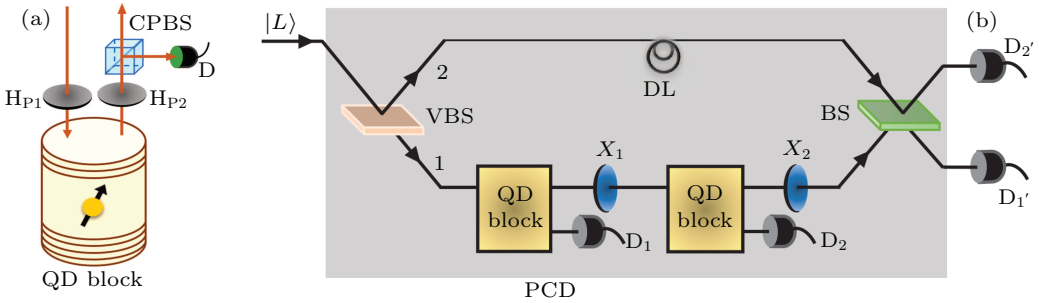



**Fig. 2.** (a) Schematic diagram of the error-heralded QD block. (b) Schematic diagram of error-heralded parity-check device (PCD) on electron-spin system. $H_{Pi}$ $(i = 1, 2)$ is a half-wave plate that performs Hadamard operation on the photon, *i.e.*, $|R\rangle \to (|R\rangle + |L\rangle)/\sqrt{2}$, and $|L\rangle \to (|R\rangle - |L\rangle)/\sqrt{2}$. CPBS represents a circular polarization beam splitter, which transmits a right-polarized photon $|R\rangle$ and reflects a left-polarized photon $|L\rangle$. $D_j$ $(j = 1, 2, 1', 2')$ is a single-photon detector. VBS represents a non-equilibrium beam splitter with a transmission coefficient of $(1+P^4)^{-1/2}$ and a reflection coefficient of $P^2/[(1+P^4)]^{1/2}$. BS is a 50 : 50 beam splitter. $X_k$ $(k = 1, 2)$ is a half-wave plate, which performs bit-flip operation on the photon $\sigma_x^p = |R\rangle\langle L| + |L\rangle\langle R|$.

During the single photon scattering processes, if the photon is reflected by the error-heralded QD-cavity block, it will trigger the detector either $D_1$ or $D_2$, which means the failure of the PCD. In detail, when the single photon detector $D_1$ triggers, the error occurs in the parity measurement task of this round, another single photon can be input to complete the parity outcome of the two-electron spins. On the premise of ignoring the photon scattering with inherent losses channeled into its environment in first QD block, the photon passes through the half-wave plate $X_1$ when the $D_1$ does not respond. When the single photon detector $D_2$ responds, after the phase-flip operation $\sigma_x^e = |\uparrow\rangle\langle\uparrow| - |\downarrow\rangle\langle\downarrow|$ on the second electron spin, another single photon is input. If the input photon is transmitted through the two error-heralded QD blocks, there is no click of the single-photon detector $D_1$ or $D_2$. At last, the two modes of the photon, passing though different optical paths, will come together again through the BS and be detected, completing the PCD of the two-electron spins. The BS performs operations

$$\frac{1}{\sqrt{2}}(|L\rangle_2 + |L\rangle_1) \to |L\rangle_{2'}, \quad \frac{1}{\sqrt{2}}(|L\rangle_2 - |L\rangle_1) \to |L\rangle_{1'}. \tag{8}$$

The evolutions of the whole system consisting of two-electron spins and the injected photon are described as

$$|\phi^\pm\rangle|L\rangle \xrightarrow{\text{PCD}} \beta|\phi^\pm\rangle|L\rangle_{2'}, \quad |\psi^\pm\rangle|L\rangle \xrightarrow{\text{PCD}} \beta|\psi^\pm\rangle|L\rangle_{1'}, \tag{9}$$

where $\beta = [2P^4/(1+P^4)]^{1/2}$. $|L\rangle_{2'}$ $(|L\rangle_{1'})$ means that the photon is detected by $D_{2'}$ $(D_{1'})$. If $D_{2'}$ $(D_{1'})$ responds, the two-electron spins are even (odd) parity. The PCD is established to perform our MEPP.

## 3. High-efficiency three-electron-spin EPP for bit-flip errors

For three-electron-spin entangled states, there are eight GHZ states written as follows:

$$|\phi_0^\pm\rangle_{ABC} = \frac{1}{\sqrt{2}}(|\uparrow\uparrow\uparrow\rangle \pm |\downarrow\downarrow\downarrow\rangle)_{ABC},$$

$$|\phi_1^{\pm}\rangle_{ABC} = \frac{1}{\sqrt{2}}(|\downarrow\uparrow\uparrow\rangle \pm |\uparrow\downarrow\downarrow\rangle)_{ABC},$$
$$|\phi_2^{\pm}\rangle_{ABC} = \frac{1}{\sqrt{2}}(|\uparrow\downarrow\uparrow\rangle \pm |\downarrow\uparrow\downarrow\rangle)_{ABC},$$
$$|\phi_3^{\pm}\rangle_{ABC} = \frac{1}{\sqrt{2}}(|\uparrow\uparrow\downarrow\rangle \pm |\downarrow\downarrow\uparrow\rangle)_{ABC}. \quad (10)$$

Here, the subscripts $A$, $B$, and $C$ denote the three-electron spins sent to Alice, Bob, and Charlie, respectively. Suppose that the original three-electron-spin GHZ state transmitted among the three parties is $|\phi_0^+\rangle_{ABC}$. As we know, the noisy channel will inevitably change a pure entangled state ensemble into a mixed one. In other words, when the initial $|\phi_0^+\rangle_{ABC}$ turns into $|\phi_i^+\rangle_{ABC}$ by taking place a bit-flip error on the $i$-th $(i = 1,2,3)$ qubit, meanwhile $|\phi_0^+\rangle_{ABC}$ evolves to $|\phi_0^-\rangle_{ABC}$ due to appearing a phase-flip error. Sometimes, both a bit-flip error and a phase-flip error will take place on the three-electron-spin system with the state $|\phi_i^-\rangle_{ABC}$. Generally, a phase-flip error can be transformed into a bit-flip error assisted by a bilateral local operation. Therefore, we only discuss the MEPP for bit-flip errors of three-electron-spin mixed states in detail.

Suppose that Alice, Bob, and Charlie share a three-electron-spin ensemble $\rho$ after the transmission of qubits over the noisy channels,

$$\rho = f_0|\phi_0^+\rangle\langle\phi_0^+| + f_1|\phi_1^+\rangle\langle\phi_1^+| + f_2|\phi_2^+\rangle\langle\phi_2^+| + f_3|\phi_3^+\rangle\langle\phi_3^+|. \quad (11)$$

Here, $f_0 = \langle\phi_0^+|\rho|\phi_0^+\rangle$ is the fidelity of the quantum systems passed through noisy channels, and satisfies $f_0 + f_1 + f_2 + f_3 = 1$. The density matrix $\rho$ means that there is a bit-flip error on the $i$-th $(i = 1,2,3)$ electron spin of the quantum system with a probability of $f_i$ $(i = 1,2,3)$. For obtaining some high-fidelity entangled three-electron-spin entangled systems, three parties need a pair of three-electron-spin quantum systems with $A_1B_1C_1$ and $A_2B_2C_2$, respectively. Then, the state of six-electron-spin system $\rho_{A_1B_1C_1} \otimes \rho_{A_2B_2C_2}$ can be viewed as the mixture of the sixteen pure states, *i.e.*, $|\phi_i^+\rangle \otimes |\phi_j^+\rangle$ with the probability of $f_i f_j$ $(i, j = 0,1,2,3)$. Here, the electron-spin with subscripts $A_1$ and $A_2$ belong to Alice, $B_1$ and $B_2$ belong to Bob, and $C_1$ and $C_2$ belong to Charlie. Our efficient MEPP for three-electron-spin entangled systems with the bit-flip errors is divided into two purified steps.

### 3.1. The first step of three-electron-spin EPP for bit-flip errors with PCDs

The process of the first step of our MEPP is shown in Fig. 3(a). The left-circular-polarized states $|L\rangle_A$, $|L\rangle_B$, and $|L\rangle_C$ are injected into the quantum circuit by Alice, Bob, and Charlie, respectively. At first three parts perform the PCDs on two-electron spins $A_1A_2$, $B_1B_2$, and $C_1C_2$, respectively, and then measure the electron spins $A_2$, $B_2$, $C_2$, respectively, with the basis $M_X$, *i.e.*, $|+\rangle = \frac{1}{\sqrt{2}}(|\uparrow\rangle + |\downarrow\rangle)$, and $|-\rangle = \frac{1}{\sqrt{2}}(|\uparrow\rangle - |\downarrow\rangle)$, which is equivalent to performing a Hadamard gate on the electron spin using a $\pi/2$ microwave pulse.[56,57]

(i) Three parties compare the parity outcomes of their thtee electron-spin pairs with PCDs. If Alice, Bob, and Charlie can get the same parity-mode outcome as each other, which corresponds to the identity-combination terms $|\phi_i^+\rangle \otimes |\phi_j^+\rangle$ $(i = j \in \{0,1,2,3\})$, they keep their two electron-spin pairs. The same parity-mode outcome can be divided into two groups. If the injected three photons trigger the upper detectors $D_{A2'}$, $D_{B2'}$, and $D_{C2'}$, the entangled electron-spin systems collapse to four even-parity states as follows:

$$\begin{aligned}
|\Phi_0\rangle &= \frac{1}{\sqrt{2}}(|\uparrow\uparrow\uparrow\rangle_{A_1B_1C_1}|\uparrow\uparrow\uparrow\rangle_{A_2B_2C_2} + |\downarrow\downarrow\downarrow\rangle_{A_1B_1C_1}|\downarrow\downarrow\downarrow\rangle_{A_2B_2C_2}),\\
|\Phi_1\rangle &= \frac{1}{\sqrt{2}}(|\downarrow\uparrow\uparrow\rangle_{A_1B_1C_1}|\downarrow\uparrow\uparrow\rangle_{A_2B_2C_2} + |\uparrow\downarrow\downarrow\rangle_{A_1B_1C_1}|\uparrow\downarrow\downarrow\rangle_{A_2B_2C_2}),\\
|\Phi_2\rangle &= \frac{1}{\sqrt{2}}(|\uparrow\downarrow\uparrow\rangle_{A_1B_1C_1}|\uparrow\downarrow\uparrow\rangle_{A_2B_2C_2} + |\downarrow\uparrow\downarrow\rangle_{A_1B_1C_1}|\downarrow\uparrow\downarrow\rangle_{A_2B_2C_2}),\\
|\Phi_3\rangle &= \frac{1}{\sqrt{2}}(|\uparrow\uparrow\downarrow\rangle_{A_1B_1C_1}|\uparrow\uparrow\downarrow\rangle_{A_2B_2C_2} + |\downarrow\downarrow\uparrow\rangle_{A_1B_1C_1}|\downarrow\downarrow\uparrow\rangle_{A_2B_2C_2}). \quad (12)
\end{aligned}$$

In contrast, if the injected three photons trigger the lower detectors $D_{A1'}$, $D_{B1'}$, and $D_{C1'}$, the entangled electron-spin systems collapse to four odd-parity states as follows:

$$\begin{aligned}
|\Psi_0\rangle &= \frac{1}{\sqrt{2}}(|\uparrow\uparrow\uparrow\rangle_{A_1B_1C_1}|\downarrow\downarrow\downarrow\rangle_{A_2B_2C_2} + |\downarrow\downarrow\downarrow\rangle_{A_1B_1C_1}|\uparrow\uparrow\uparrow\rangle_{A_2B_2C_2}),\\
|\Psi_1\rangle &= \frac{1}{\sqrt{2}}(|\downarrow\uparrow\uparrow\rangle_{A_1B_1C_1}|\uparrow\downarrow\downarrow\rangle_{A_2B_2C_2} + |\uparrow\downarrow\downarrow\rangle_{A_1B_1C_1}|\downarrow\uparrow\uparrow\rangle_{A_2B_2C_2}),\\
|\Psi_2\rangle &= \frac{1}{\sqrt{2}}(\uparrow\downarrow\uparrow\rangle_{A_1B_1C_1}|\downarrow\uparrow\downarrow\rangle_{A_2B_2C_2} + |\downarrow\uparrow\downarrow\rangle_{A_1B_1C_1}|\uparrow\downarrow\uparrow\rangle_{A_2B_2C_2}),\\
|\Psi_3\rangle &= \frac{1}{\sqrt{2}}(|\uparrow\uparrow\downarrow\rangle_{A_1B_1C_1}|\downarrow\downarrow\uparrow\rangle_{A_2B_2C_2} + |\downarrow\downarrow\uparrow\rangle_{A_1B_1C_1}|\uparrow\uparrow\downarrow\rangle_{A_2B_2C_2}). \quad (13)
\end{aligned}$$

The states $|\Psi_0\rangle$, $|\Psi_1\rangle$, $|\Psi_2\rangle$, and $|\Psi_3\rangle$ can be transformed into $|\Phi_0\rangle$, $|\Phi_1\rangle$, $|\Phi_2\rangle$, and $|\Phi_3\rangle$ by a bit-flip operation $\sigma_x^e = |\uparrow\rangle\langle\downarrow| + |\downarrow\rangle\langle\uparrow|$ on the electron spin $A_2$, $B_2$, and $C_2$, respectively. Subsequently, Alice, Bob, and Charlie measure with the basis $M_X = \{|+\rangle, |-\rangle\}$ on the electron spin $A_2$, $B_2$, and $C_2$, respectively. The states $|\Phi_0\rangle$, $|\Phi_1\rangle$, $|\Phi_2\rangle$, and $|\Phi_3\rangle$ can be changed into the states $|\Phi_0'\rangle$, $|\Phi_1'\rangle$, $|\Phi_2'\rangle$, and $|\Phi_3'\rangle$, respectively. Here,

$$\begin{aligned}
|\Phi_0'\rangle = \frac{1}{4}[&|\phi_0^+\rangle_{A_1B_1C_1}(|++\rangle + |+-\rangle + |-+\rangle + |--+\rangle)_{A_2B_2C_2}\\
&+|\phi_0^-\rangle_{A_1B_1C_1}(|++-\rangle + |+-+\rangle + |-++\rangle + |---\rangle)_{A_2B_2C_2}],
\end{aligned}$$

$$
\begin{aligned}
|\Phi_1'\rangle &= \frac{1}{4}[|\phi_1^+\rangle_{A_1B_1C_1}(|+++\rangle+|+--\rangle \\
&\quad -|-+-\rangle-|--+\rangle)_{A_2B_2C_2} \\
&\quad +|\phi_1^-\rangle_{A_1B_1C_1}(|++-\rangle+|+-+\rangle \\
&\quad -|-++\rangle-|---\rangle)_{A_2B_2C_2}], \\
|\Phi_2'\rangle &= \frac{1}{4}[|\phi_2^+\rangle_{A_1B_1C_1}(|+++\rangle-|+--\rangle \\
&\quad +|-+-\rangle-|--+\rangle)_{A_2B_2C_2} \\
&\quad +|\phi_2^-\rangle_{A_1B_1C_1}(|++-\rangle-|+-+\rangle \\
&\quad +|-++\rangle-|---\rangle)_{A_2B_2C_2}], \\
|\Phi_3'\rangle &= \frac{1}{4}[|\phi_3^+\rangle_{A_1B_1C_1}(|+++\rangle-|+--\rangle \\
&\quad -|-+-\rangle+|--+\rangle)_{A_2B_2C_2} \\
&\quad +|\phi_3^-\rangle_{A_2B_1C_1}(|++-\rangle-|+-+\rangle \\
&\quad -|-++\rangle+|---\rangle)_{A_2B_2C_2}]. \qquad (14)
\end{aligned}
$$

Obviously, the results can be divided into two groups considering the number of $|-\rangle$. If the number of the outcomes $|-\rangle$ is even, Alice, Bob, and Charlie obtain the GHZ states $|\phi_0^+\rangle_{A_1B_1C_1}$, $|\phi_1^+\rangle_{A_1B_1C_1}$, $|\phi_2^+\rangle_{A_1B_1C_1}$, and $|\phi_3^+\rangle_{A_1B_1C_1}$ with the probabilities $\frac{1}{2}f_0^2$, $\frac{1}{2}f_1^2$, $\frac{1}{2}f_2^2$, and $\frac{1}{2}f_3^2$, respectively. Otherwise, if the number of the outcomes $|-\rangle$ is odd and the three parties obtain the other four states $|\phi_0^-\rangle_{A_1B_1C_1}$, $|\phi_1^-\rangle_{A_1B_1C_1}$, $|\phi_2^-\rangle_{A_1B_1C_1}$, and $|\phi_3^-\rangle_{A_1B_1C_1}$ with the probabilities $\frac{1}{2}f_0^2$, $\frac{1}{2}f_1^2$, $\frac{1}{2}f_2^2$, and $\frac{1}{2}f_3^2$, respectively. Alice, Bob, and Charlie can transform the states $|\phi_0^-\rangle$, $|\phi_1^-\rangle$, $|\phi_2^-\rangle$, and $|\phi_3^-\rangle$ into the states $|\phi_0^+\rangle$, $|\phi_1^+\rangle$, $|\phi_2^+\rangle$, and $|\phi_3^+\rangle$ with a phase-flip operation $\sigma_x^e$ on the first electron spin $A_1$, $B_1$, and $C_1$, respectively. Therefore, Alice, Bob, and Charlie can obtain the three-electron-spin maximally entangled states obtained from ideal-combination items $|\phi_i^+\rangle_{A_1B_1C_1}\otimes|\phi_j^+\rangle_{A_2B_2C_2}$ $(i=j\in\{0,1,2,3\})$ and the corresponding probability, as shown in Table 1, which are only one bit-flip error taking place. That is, by keeping the instances in which all the three parties obtain the same output modes, and then measuring the number of $|-\rangle$, Alice, Bob, and Charlie can obtain a new three-electron-spin ensemble in the state

$$
\begin{aligned}
\rho'_{A_1B_1C_1} &= f_0'|\phi_0^+\rangle\langle\phi_0^+|+f_1'|\phi_1^+\rangle\langle\phi_1^+| \\
&\quad +f_2'|\phi_2^+\rangle\langle\phi_2^+|+f_3'|\phi_3^+\rangle\langle\phi_3^+|, \qquad (15)
\end{aligned}
$$

where $f_0'=f_0^2/(f_0^2+f_1^2+f_2^2+f_3^2)$, $f_1'=f_1^2/(f_0^2+f_1^2+f_2^2+f_3^2)$, $f_2'=f_2^2/(f_0^2+f_1^2+f_2^2+f_3^2)$, and $f_3'=f_3^2/(f_0^2+f_1^2+f_2^2+f_3^2)$. The fidelity $f_0'>f_0$ if $f_0$ satisfies the relation $f_0>\{3-2f_1-2f_2-[1+4(f_1+f_2)-12(f_1^2+f_2^2)-8f_1f_2]^{1/2}\}/4$. With three symmetric noisy channels $f_1=f_2=f_3<f_0$, the fidelity of the state $|\phi_0^+\rangle$ will be improved when its original fidelity $f_0>0.25$.

**Table 1.** The states of the three-electron-spin systems obtained from identity-combination items and the corresponding probabilities (suppose $x=A_1B_1C_1$ and $y=A_2B_2C_2$ for simplification).

| Identity-combination items | $\|\phi_0^+\rangle_x\otimes\|\phi_0^+\rangle_y$ | $\|\phi_1^+\rangle_x\otimes\|\phi_1^+\rangle_y$ | $\|\phi_2^+\rangle_x\otimes\|\phi_2^+\rangle_y$ | $\|\phi_3^+\rangle_x\otimes\|\phi_3^+\rangle_y$ |
|---|---|---|---|---|
| Three-electron-spin states | $\|\phi_0^+\rangle_x$ | $\|\phi_1^+\rangle_x$ | $\|\phi_2^+\rangle_x$ | $\|\phi_3^+\rangle_x$ |
| Probabilities | $f_0^2$ | $f_1^2$ | $f_2^2$ | $f_3^2$ |

(ii) In the above three-electron-spin EPP for bit-flip errors, the three parties obtain different parity-mode outputs, which are not taken into consideration, *i.e.*, the cross-combination terms $|\phi_i^+\rangle\otimes|\phi_j^+\rangle$ $(i\neq j\in\{0,1,2,3\})$, as the item $|\phi_j^+\rangle_{A_1B_1C_1}\otimes|\phi_i^+\rangle_{A_2B_2C_2}$ has the same probability $f_if_j$ to the item $|\phi_i^+\rangle_{A_1B_1C_1}\otimes|\phi_j^+\rangle_{A_2B_2C_2}$, $(i\neq j\in\{0,1,2,3\})$. However, they can utilize the cross-combination items to produce some high-fidelity two-electron-spin entangled states. To be detail, we take the cross-combination terms $|\phi_0^+\rangle_{A_1B_1C_1}\otimes|\phi_2^+\rangle_{A_2B_2C_2}$ and $|\phi_2^+\rangle_{A_1B_1C_1}\otimes|\phi_0^+\rangle_{A_2B_2C_2}$ as an example to discuss. As for the others, we could deal with them in the same way with or without a little modification. With PCDs, two parts obtain the same parity modes as each other when they measure their photons, we keep their two electron-spin pairs. If the injected three photons trigger the upper detectors $D_{A2'}$, $D_{C2'}$, and the lower one $D_{B1'}$, the six-electron-spin entangled systems collapse into the quantum states as follows:

$$
\begin{aligned}
|\Omega_1\rangle &= \frac{1}{\sqrt{2}}(|\uparrow\uparrow\uparrow\rangle_{A_1B_1C_1}|\uparrow\downarrow\uparrow\rangle_{A_2B_2C_2} \\
&\quad +|\downarrow\downarrow\downarrow\rangle_{A_1B_1C_1}|\downarrow\uparrow\downarrow\rangle_{A_2B_2C_2}), \\
|\Omega_2\rangle &= \frac{1}{\sqrt{2}}(|\uparrow\downarrow\uparrow\rangle_{A_1B_1C_1}|\uparrow\uparrow\uparrow\rangle_{A_2B_2C_2} \\
&\quad +|\downarrow\uparrow\downarrow\rangle_{A_1B_1C_1}|\downarrow\downarrow\downarrow\rangle_{A_2B_2C_2}). \qquad (16)
\end{aligned}
$$

In contrast, if the injected three photons trigger the lower detectors $D_{A1'}$, $D_{C1'}$, and the upper one $D_{B2'}$, the six-electron-spin entangled systems collapse into the quantum states as follows:

$$
\begin{aligned}
|\Omega_3\rangle &= \frac{1}{\sqrt{2}}(|\uparrow\uparrow\uparrow\rangle_{A_1B_1C_1}|\downarrow\uparrow\downarrow\rangle_{A_2B_2C_2} \\
&\quad +|\downarrow\downarrow\downarrow\rangle_{A_1B_1C_1}|\uparrow\downarrow\uparrow\rangle_{A_2B_2C_2}), \\
|\Omega_4\rangle &= \frac{1}{\sqrt{2}}(|\uparrow\downarrow\uparrow\rangle_{A_1B_1C_1}|\downarrow\downarrow\downarrow\rangle_{A_2B_2C_2} \\
&\quad +|\downarrow\uparrow\downarrow\rangle_{A_1B_1C_1}|\uparrow\uparrow\uparrow\rangle_{A_2B_2C_2}). \qquad (17)
\end{aligned}
$$

That is, Alice, Bob, and Charlie can acquire a high-fidelity two-electron-spin entangled state $|\phi^+\rangle_{A_1C_1}$ from the six-electron-spin state $|\Omega_1\rangle$. In detail, Alice and Charlie measure their electron spins $A_2$ and $C_2$, respectively, and Bob measures two-electron spins $B_1$ and $B_2$ with the basis $M_X=\{|+\rangle,|-\rangle\}$. The states $|\Omega_1\rangle$ can be changed into the states $|\Omega_1'\rangle$. Here,

$$
\begin{aligned}
|\Omega'\rangle_1 &= \frac{1}{2}[|\phi^+\rangle_{A_1C_1}(|++++\rangle-|++--\rangle \\
&\quad +|+-+-\rangle-|+--+\rangle
\end{aligned}
$$

$$
\begin{aligned}
&+|-++-\rangle-|-+-+\rangle\\
&+|--++\rangle-|----\rangle_{A_2C_2B_1B_2}\\
&+|\phi^-\rangle_{A_1C_1}(|+++-\rangle-|++-+\rangle\\
&+|+-++\rangle-|+---\rangle\\
&+|-+++\rangle-|-+--\rangle\\
&+|--+-\rangle-|---+\rangle)_{A_2C_2B_1B_2})]. \qquad (18)
\end{aligned}
$$

Alice and Charlie obtain the two-electron-spin entangled state $|\phi^+\rangle_{A_1C_1}$ when the number of the outcomes $|-\rangle$ is even. When the number of the outcomes $|-\rangle$ is odd, Alice and Charlie obtain the two-electron-spin entangled state $|\phi^-\rangle_{A_1C_1}$ and they can transform the state $|\phi^-\rangle_{A_1C_1}$ into the state $|\phi^+\rangle_{A_1C_1}$ by performing a phase-flip operation $\sigma_x^e$ on the electron $C_1$. For the other three states $|\Omega_i\rangle$ $(i=2,3,4)$, Alice, Bob, and Charlie can also obtain the two-electron-spin entangled state $|\phi^+\rangle_{A_1C_1}$ with the same principle. That is, three parts can obtain the two-electron-spin maximally entangled state $|\phi^+\rangle_{A_1C_1}$ from the cross-combination terms $|\phi_0^+\rangle_{A_1B_1C_1}\otimes|\phi_2^+\rangle_{A_2B_2C_2}$ and $|\phi_2^+\rangle_{A_1B_1C_1}\otimes|\phi_0^+\rangle_{A_2B_2C_2}$ with the probability of $2f_0f_2$. In the same way, Alice, Bob, and Charlie can obtain the two-electron-spin maximally entangled states $|\psi^+\rangle_{A_1B_1}$, $|\psi^+\rangle_{A_1C_1}$ and $|\psi^+\rangle_{B_1C_1}$ from the cross-combination terms $|\phi_i^+\rangle_{A_1B_1C_1}\otimes|\phi_j^+\rangle_{A_2B_2C_2}$ $(i\neq j\in\{0,1,2,3\})$, and the corresponding probability shown in Table 2. The total states of the two-electron-spin systems could be described as

$$
\begin{aligned}
\rho_{A_1B_1} &= 2f_0f_3|\phi^+\rangle_{A_1B_1}\langle\phi^+|+2f_1f_2|\psi^+\rangle_{A_1B_1}\langle\psi^+|,\\
\rho_{A_1C_1} &= 2f_0f_2|\phi^+\rangle_{A_1C_1}\langle\phi^+|+2f_1f_3|\psi^+\rangle_{A_1C_1}\langle\psi^+|,\\
\rho_{B_1C_1} &= 2f_0f_1|\phi^+\rangle_{B_1C_1}\langle\phi^+|+2f_2f_3|\psi^+\rangle_{B_1C_1}\langle\psi^+|. \qquad (19)
\end{aligned}
$$

Provided that $f_1=f_2=f_3$, and $f_0>f_1$, the density matrices in Eq. (19) can simplify

$$
\begin{aligned}
\rho'_{AB} &= f'_0|\phi^+\rangle_{AB}\langle\phi^+|+f'_1|\psi^+\rangle_{AB}\langle\psi^+|,\\
\rho'_{AC} &= f'_0|\phi^+\rangle_{AC}\langle\phi^+|+f'_1|\psi^+\rangle_{AC}\langle\psi^+|,\\
\rho'_{BC} &= f'_0|\phi^+\rangle_{BC}\langle\phi^+|+f'_1|\psi^+\rangle_{BC}\langle\psi^+|, \qquad (20)
\end{aligned}
$$

where $f'_0=f_0/(f_0+f_1)$, and $f'_1=f_1/(f_0+f_1)$. Further, one can see that the purified fidelity of two-electron-spin systems is larger than that of the original three-electron-spin systems transmitted. For example, $f(|\phi^+\rangle_{AB})=f'_0>f_0$ under the condition $f_0+f_1<1$. The first step of the first round of the MEPP process is accomplished.

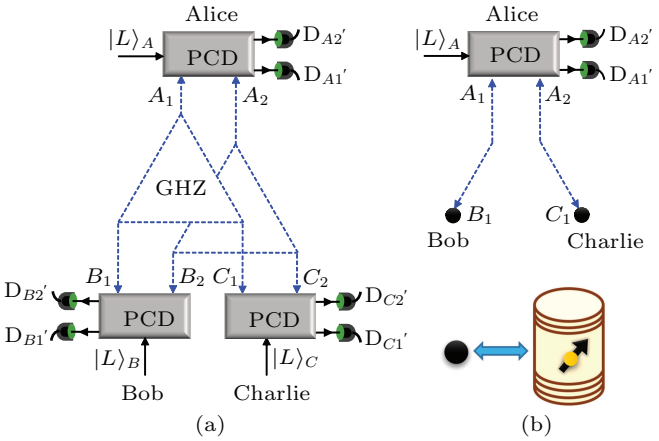



**Fig. 3.** (a) The principle of the first step of our three-electron-spin EPP for bit-flip errors with parity-check devices (PCDs). (b) The principle of the entanglement link for reproducing a three-electron-spin entangled system from two two-electron-spin entangled systems. $D_j$ $(j=A1',A2',B1',B2',C1',C2')$ represent a single-photon detector. The black symbol '•' represents a QD spin.

**Table 2.** The states of the two electron-spin systems obtained from the cross-combination terms and the corresponding probabilities (suppose that $x=A_1B_1C_1$ and $y=A_2B_2C_2$ for simplification).

| | | | |
|---|---|---|---|
| Cross-combination terms | $\|\phi_0^+\rangle_x\otimes\|\phi_2^+\rangle_y$<br>$\|\phi_2^+\rangle_x\otimes\|\phi_0^+\rangle_y$ | $\|\phi_0^+\rangle_x\otimes\|\phi_1^+\rangle_y$<br>$\|\phi_1^+\rangle_x\otimes\|\phi_0^+\rangle_y$ | $\|\phi_0^+\rangle_x\otimes\|\phi_3^+\rangle_y$<br>$\|\phi_3^+\rangle_x\otimes\|\phi_0^+\rangle_y$ |
| Two-electron-spin states | $\|\phi^+\rangle_{A_1C_1}$ | $\|\phi^+\rangle_{B_1C_1}$ | $\|\phi^+\rangle_{A_1B_1}$ |
| Probabilities | $2f_0f_2$ | $2f_0f_1$ | $2f_0f_3$ |
| Cross-combination terms | $\|\phi_1^+\rangle_x\otimes\|\phi_2^+\rangle_y$<br>$\|\phi_2^+\rangle_x\otimes\|\phi_1^+\rangle_y$ | $\|\phi_1^+\rangle_x\otimes\|\phi_3^+\rangle_y$<br>$\|\phi_3^+\rangle_x\otimes\|\phi_1^+\rangle_y$ | $\|\phi_2^+\rangle_x\otimes\|\phi_3^+\rangle_y$<br>$\|\phi_3^+\rangle_x\otimes\|\phi_2^+\rangle_y$ |
| Two-electron-spin states | $\|\psi^+\rangle_{A_1B_1}$ | $\|\psi^+\rangle_{A_1C_1}$ | $\|\psi^+\rangle_{B_1C_1}$ |
| Probabilities | $2f_1f_2$ | $2f_1f_3$ | $2f_2f_3$ |

### 3.2. The second step of three-electron-spin EPP for bit-flip errors with HL

Now the detail principle reproducing three-electron-spin entangled systems from the above two-electron-spin entangled systems with entanglement link (HL) will be presented here. As discussed above, the two-electron spin in the original system are symmetric to each other, we can exploit $\rho_{A_1B_1}$ and $\rho_{A_2C_1}$ as an example to describe the principle shown in Fig. 3(b). The system composed of the four-electron spin $A_1B_1A_2C_1$ is in the state $\rho'_{A_1B_1}\otimes\rho'_{A_2C_1}$, which can be viewed as the mixture of the four pure states $|\phi^+\rangle_{A_1B_1}\otimes|\phi^+\rangle_{A_2C_1}$, $|\phi^+\rangle_{A_1B_1}\otimes|\psi^+\rangle_{A_2C_1}$, $|\psi^+\rangle_{A_1B_1}\otimes|\phi^+\rangle_{A_2C_1}$, and $|\psi^+\rangle_{A_1B_1}\otimes|\psi^+\rangle_{A_2C_1}$ with the probabilities $f_0'^2$, $f'_0f'_1$, $f'_1f'_0$, and $f_1'^2$, respectively.

After Alice's PCD, they divide the four-electron-spin systems into two cases due to different parity-mode outcomes. If the parity of the two-electron spins $A_1A_2$ is even, the corresponding detector $D_{A2'}$ clicked, and then Alice detects the electron spin $A_2$ with the basis $M_X=\{|+\rangle,|-\rangle\}$, Alice, Bob, and Charlie will obtain a three-electron-spin entangled system in the states $|\phi_0^+\rangle$, $|\phi_3^+\rangle$, $|\phi_2^+\rangle$, and $|\phi_1^+\rangle$ with an auxiliary phase-flip operation $\sigma_z$ on the electron spin $A_1$. In contrast, if the parity of the two-electron spins $A_1A_2$ is odd, the corresponding detector $D_{A1'}$ clicked, and detects the electron

spin $A_2$ with the basis $M_X = \{|+\rangle, |-\rangle\}$, the three parties can acquire the same ones as the above case with a bit-flip operation $\sigma_x$ on the electron spins $A_1$ and $C_1$ independently. Similarly, Alice, Bob, and Charlie can reobtain the three-electron-spin maximally entangled states $|\phi_0^+\rangle$, $|\phi_3^+\rangle$, $|\phi_2^+\rangle$, and $|\phi_1^+\rangle$ from the cross-combination terms $|\Phi_i^+\rangle_{A_1B_1C_1} \otimes |\Phi_j^+\rangle_{A_2B_2C_2}$ $(i \neq j \in \{0,1,2,3\})$, and the corresponding probability shown in Table 3. That is, with entanglement link, Alice, Bob, and Charlie can reproduce a new ensemble for three-electron-spin systems in the state

$$\rho''_{A_1B_1C_1} = f_0''|\phi_0^+\rangle\langle\phi_0^+| + f_1''|\phi_1^+\rangle\langle\phi_1^+| + f_2''|\Phi_2^+\rangle\langle\phi_2^+| + f_3''|\phi_3^+\rangle\langle\phi_3^+|. \quad (21)$$

Here, $f_0'' = f_0^2/(f_0+f_1)^2$, $f_1'' = f_1^2/(f_0+f_1)^2$, and $f_2'' = f_3'' = f_0f_1/(f_0+f_1)^2$. The second step of the first round of the MEPP process is accomplished above. $f_0'' > f_0$ when $f_0 > 0.25$, which means that the three parties can reobtain a high-fidelity three-electron-spin entangled systems from two two-electron-spin entangled subsystems if and only if the original fidelity of the three-electron-spin systems transmitted over noisy channels is larger than 0.25.

**Table 3.** The three-electron-spin systems reobtained from two-electron-spin systems and the corresponding probabilities (suppose $p = A_1B_1$ and $q = A_2C_1$ for simplification).

| | | | | |
|---|---|---|---|---|
| Two-electron-spin states | $\|\phi^+\rangle_p \otimes \|\phi^+\rangle_q$ | $\|\phi^+\rangle_p \otimes \|\psi^+\rangle_q$ | $\|\psi^+\rangle_p \otimes \|\phi^+\rangle_q$ | $\|\psi^+\rangle_p \otimes \|\psi^+\rangle_q$ |
| Three-electron-spin states | $\|\phi_0^+\rangle_{A_1B_1C_1}$ | $\|\phi_3^+\rangle_{A_1B_1C_1}$ | $\|\phi_2^+\rangle_{A_1B_1C_1}$ | $\|\phi_1^+\rangle_{A_1B_1C_1}$ |
| Probabilities | $f_0'^2$ | $f_0'f_1'$ | $f_1'f_0'$ | $f_1'^2$ |

### 3.3. The efficiency of three-electron-spin EPP for bit-flip errors

After the above two purified steps, the first round of the MEPP process is accomplished. The purified fidelity of the three-electron-spin system $A_1B_1C_1$ can be improved further by repeating multiple rounds of the MEPP. Furthermore, the efficiency of obtaining the efficiency of three-electron-spin system $A_1B_1C_1$ after the first purification step is $\eta_1$, while the efficiency of obtaining the three-electron-spin system $A_1B_1C_1$ after introducing the second purification step with HL is $\eta_2$,

$$\eta_1 = \sum_{m=n=0}^{3} f_m f_n = \frac{1-2f_0+4f_0^2}{3},$$
$$\eta_2 = \frac{1}{2}\sum_{m\neq n=0}^{3} f_m f_n + \eta_1 = \frac{2-f_0+2f_0^2}{3}, \quad (22)$$

where $f_1 = f_2 = f_3 = (1-f_0)/3$. $\eta_1$ and $\eta_2$ are shown in Fig. 4, which easily find that the efficiency $\eta_2$ of our MEPP is greatly increased. For the initial fidelity $f_0 < 0.5$, $\eta_2$ is far larger than $2\eta_1$. Obviously, the initial fidelity $f_0$ is smaller 0.5, the second purified step with quantum HL plays an important role in the first round of the MEPP process.

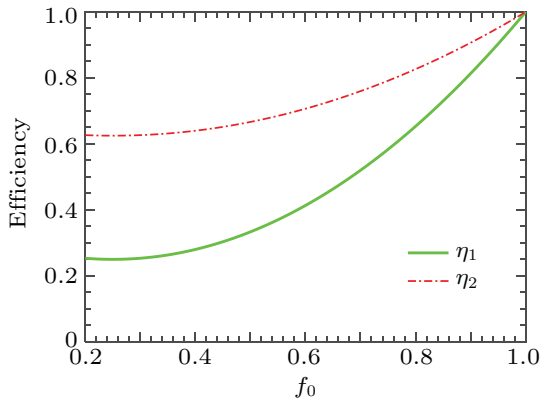



**Fig. 4.** The efficiencies $\eta_1$ and $\eta_2$ *versus* the initial fidelity $f_0$.

In addition, the efficiency $\eta_1$ of our MEPP is double as those in Refs. [48–50] due to taking all the cases in which all the parties obtain either even or odd parity into account for obtaining high-fidelity three-electron-spin entangled systems. Two purified steps are independently in the next round. That is, they can first purify two-electron-spin systems with the fidelity $f_0$ and then produce high-fidelity three-electron-spin systems with entanglement link. Besides, as all quantum operations, the PCDs and HL, will work with a near-unity fidelity, the MEPP here will be performed faithfully and work without the influence from every purified operation.

## 4. Discussion and summary

Furthermore, our three partite EPP can be directly extended to purify $N$-electron-spin entangled systems, resorting to the self-error-rejecting parity-check devices (PCDs) and entanglement link. There are $2^N$ GHZ states for an $N$-electron-spin systems and can be written as

$$|\phi_{ij\cdots k}^{\pm}\rangle_N = \frac{1}{\sqrt{2}}(|ij\cdots k\rangle \pm |\bar{i}\bar{j}\cdots\bar{k}\rangle)_{AB\cdots Z}. \quad (23)$$

Here $\bar{i} = 1-i$, $\bar{j} = 1-j$, $\bar{k} = 1-k$, and $i, j, k \in \{0,1\}$. $|0\rangle \equiv |\uparrow\rangle$ and $|1\rangle \equiv |\downarrow\rangle$. The subscripts $A$, $B$, …, and $Z$ represent the electrons sent to the parties Alice, Bob, …, and Zach, respectively. That is, let us assume that the ensemble of $N$-electron-spin systems after the transmission over a noisy channel is in the state

$$\rho_N = f_0|\phi_0^+\rangle_N\langle\phi_0^+| + \cdots + f_{ij\cdots k}|\phi_{ij\cdots k}^+\rangle_N\langle\phi_{ij\cdots k}^+| + \cdots + f_{2^{N-1}-1}|\phi_{2^{N-1}-1}^+\rangle_N\langle\phi_{2^{N-1}-1}^+|. \quad (24)$$

Here, $f_{ij\cdots k}$ presents the probability that an $N$-electron-spin systems is in the state $|\Phi_{ij\cdots k}^+\rangle_N$ and satisfies $f_0 + \cdots + f_{ij\cdots k} +$

$\cdots + f_{2^{N-1}-1} = 1$. Similarly, the whole MEPP is divided into two steps, in order to correct bit-flip errors in multipartite entangled quantum systems. The first step of the $N$-electron-spin EPP with bit-flip errors from the identity-combination terms $|\phi^+_{lr\cdots q}\rangle_N \otimes |\phi^+_{ij\cdots k}\rangle_N$ ($l = i$, $r = j$, …, or $q = k$), is similar to that for three-electron-spin EPP, which only increase the number of the PCDs and single-photon detectors shown in Fig. 3. Besides, the parties can acquire some high-fidelity $M$-electron-spin entangled systems ($2 \leq M < N$) from the cross-combination terms $|\phi^+_{lr\cdots q}\rangle_N \otimes |\phi^+_{ij\cdots k}\rangle_N$ ($l \neq i$, $r \neq j$, …, or $q \neq k$). The second step of the $N$-electron-spin EPP receives some high-fidelity $N$-electron-spin entangled systems from some high-fidelity $M$-electron-spin entangled systems ($2 \leq M < N$) with entanglement link.

However, the more number of the electron spins in each system, the more kinds of the EPP with entanglement link. Let us take four-electron-spin systems as an example, After Alice, Bob, Charlie, and Dean perform parity check with the own PCDs, respectively, they distil some three-electron-spin entangled systems and two-electron-spin entangled systems from the 56 cross-combination terms, and then obtain some four-electron-spin entangled systems with entanglement link. In detail, when the number of even parity is odd, we can achieve some three-electron-spin entangled states ($\rho'_{A_1B_1C_1}$, $\rho'_{A_1B_1D_1}$, $\rho'_{A_1C_1D_1}$, and $\rho'_{B_1C_1D_1}$). When the number of even parity is even, two-electron-spin entangled states ($\rho'_{A_1B_1}$, $\rho'_{A_1C_1}$, $\rho'_{A_1D_1}$, $\rho'_{B_1C_1}$, $\rho'_{B_1D_1}$, and $\rho'_{C_1D_1}$) are achieved. In detail, for a system composed of a three-electron-spin entangled subsystem $\rho'_{A_1B_1C_1}$ and a two-electron-spin entangled subsystem $\rho'_{A_2D_1}$, Alice, Bob, Charlie, and Dean can obtain a four-electron-spin entangled system by performing the PCD and measure on the electron-spin $A_2$ with the basis $M_X$ as shown in Fig. 5(a). Certainly, they can obtain a four-electron-spin entangled system from the complicated system composed of two three-electron-spin subsystems $\rho'_{A_1B_1C_1} \otimes \rho'_{A_2B_2D_1}$ as shown in Fig. 5(b), and three two-electron-spin entangled subsystems $\rho'_{A_1D_1} \otimes \rho'_{A_2C_1} \otimes \rho'_{B_1C_2}$ as shown in Fig. 5(c).

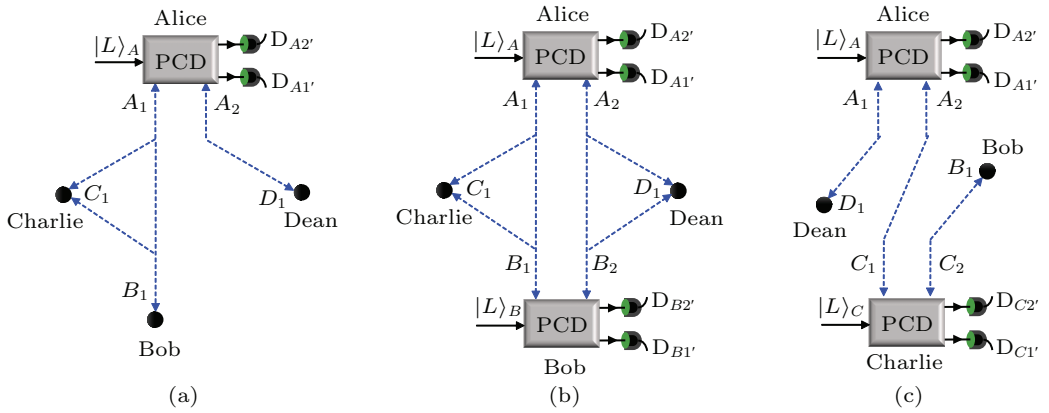



**Fig. 5.** The principle of the entanglement link for producing a four-electron spin entangled system from (a) a three-electron spin entangled subsystem and a two-electron spin entangled subsystem with a PCD, (b) two three-electron-spin entangled subsystems with two PCDs, (c) three two-electron-spin entangled subsystems with two PCDs.

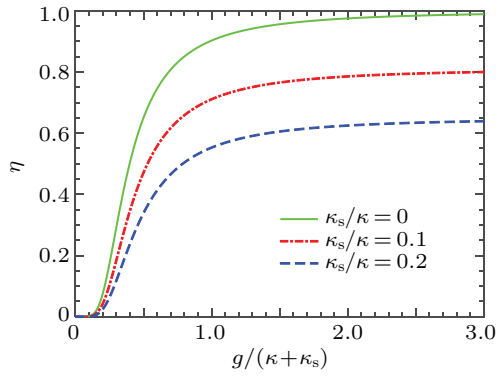



**Fig. 6.** The efficiency $\eta$ of error-heralded PCD in the case $\kappa_s/\kappa = 0$, $\kappa_s/\kappa = 0.1$, and $\kappa_s/\kappa = 0.2$ represented by the green solid line, the red dot–dash line, and the blue dot line, respectively, with $\omega = \omega_c = \omega_{X^-}$ and $\gamma/\kappa = 0.1$.

We construct the self-error-rejecting non-destructive PCD by using the error-heralded QD blocks. During the measurement process, if there is an error, the detector either $D_1$ or $D_2$ responds, and the parity outcome of electron-spin quantum state can be repeated until success. If the detector $D'_1$ or $D'_2$ responds, the parity outcome of PCD is successful. The fidelity of the PCD is robust, and immunes to the coupling strength $g$, the microcavity decay rate $\kappa$, the microcavity leakage rate $\kappa_s$ and the exciton decay rates of $\gamma$, which reduces the requirements for the experimental conditions of the scheme. However, the efficiency $\eta = \beta^2 = 2P^4/(1+P^4)$ of PCD is largely affected by the all this mentioned above factors, as shown in Fig. 6. In the case of $\omega = \omega_c = \omega_{X^-}$, $\gamma/\kappa = 0.1$, and $g/(\kappa+\kappa_s) > 2$, the efficiency becomes $\eta > 97.52\%$, $\eta > 78.55\%$, and $\eta > 62.48\%$, respectively, in the condition $\kappa_s/\kappa = 0$, $\kappa_s/\kappa = 0.1$, and $\kappa_s/\kappa = 0.2$, respectively. Furthermore, the efficiency $\eta$ could be further improved via increasing the effective QD-cavity coupling $g/(\kappa+\kappa_s)$ and decreasing the side leakage $\kappa_s/\kappa$ of the cavity.

In summary, we have proposed a high-efficiency MEPP for $N$-electron-spin systems in the GHZ state, resorting to fidelity-robust PCDs and entanglement link, which contains two steps. One is the MEPP with fidelity-robust PCDs to obtain not only high-fidelity $N$-electron-spin entangled systems

directly from ideality-combination items $|\phi^+_{lr\ldots q}\rangle_N \otimes |\phi^+_{ij\ldots k}\rangle_N$ ($l = i$, $r = j$, …, or $q = k$), but also high-fidelity $M$-electron-spin entangled subsystems ($2 \leq M < N$) from the cross-combination terms $|\phi^+_{lr\ldots q}\rangle_N \otimes |\phi^+_{ij\ldots k}\rangle_N$ ($l \neq i$, $r \neq j$, …, or $q \neq k$). The other is the recycling MEPP to regain the $N$-electron-spin entangled systems from entangled $M$-electron-spin entangled states with entanglement link. In essence, the parties distill some multipartite entangled systems from the cases which are discarded in all existing MEPPs,[48–50] which makes our MEPP have a higher efficiency. Moreover, two purified steps of our MEPP are independently in the next round, which can be carried out simultaneously to economize operation time. Further, the quantum circuits, fidelity-robust PCDs make this MEPP works faithfully, as the errors coming from practical scattering are converted into a detectable failure rather than infidelity. The fidelity-robust quantum circuits could be used directly in the failure-heralded quantum computing and quantum networks.

## Acknowledgements

Project supported in part by the National Natural Science Foundation of China (Grant No. 61901420), the Shanxi Provincial Science Foundation for Youths (Grant No. 201901D211235), and the Scientific and Technological Innovation Program of Higher Education Institutions of Shanxi Province, China (Grant No. 2019L0507).

## References

[1] Nielsen M A and Chuang I 2002 *Am. J. Phys.* **70** 558
[2] Cao H, Ma W P, Liu G, Lü L D and Xue Z Y 2020 *Chin. Phys. Lett.* **37** 050303
[3] Ke Z J, Wang Y T, Yu S, Liu W, Meng Y, Li Z P, Wang H, Li Q, Xu J S, Xiao Y, Tang J S, Li C F and Guo G C 2020 *Chin. Phys. B* **29** 080301
[4] Yang L, Liu Y C and Li Y S 2020 *Chin. Phys. B* **29** 060301
[5] Ekert A K 1991 *Phys. Rev. Lett.* **67** 661
[6] Zhao Y B, Zhang W L, Wang D, Song X T, Zhou L J and Ding C B 2019 *Chin. Phys. B* **28** 104203
[7] Cui Z X, Zhong W, Zhou L and Sheng Y B 2019 *Sci. China Phys. Mech. Astron.* **62** 110311
[8] Li J J, Wang Y, Li H W and Bao W S 2020 *Chin. Phys. B* **29** 030303
[9] Li X, Yuan H W, Zhang C M and Wang Q 2020 *Chin. Phys. B* **29** 070303
[10] Chen X T, Zhang L P, Chang S K, Zhang H and Hu L Y 2021 *Chin. Phys. B* **30** 060304
[11] Long G L and Liu X S 2002 *Phys. Rev. A* **65** 032302
[12] Zhang W, Ding D S, Sheng Y B, Zhou L, Shi B S and Guo G C 2017 *Phys. Rev. Lett.* **118** 220501
[13] Zhu F, Zhang W, Sheng Y B and Huang Y D 2017 *Sci. Bull.* **62** 1519
[14] Gao Z K, Li T and Li Z H 2019 *Europhys. Lett.* **125** 40004
[15] Li T and Long G L 2020 *New J. Phys.* **22** 063017
[16] Qi Z T, Li Y H, Huang Y W, Feng J, Zheng Y L and Chen X F 2021 *Light Sci. Appl.* **10** 183
[17] Long G L and Zhang H R 2021 *Sci. Bull.* **66** 1267
[18] Sheng Y B, Zhou L and Long G L 2021 *Sci. Bull.* **11** 002
[19] Liu X, Li Z J, Luo D, Huang C F, Ma D, Geng M M, Wang J W, Zhang Z R and Wei K J 2021 *Sci. China Phys. Mech. Astron* **64** 120311
[20] Hillery M, Bužek V and Berthiaume A 1999 *Phys. Rev. A* **59** 1829
[21] Luo G F, Zhou R G and Hu W W 2019 *Chin. Phys. B* **28** 040302
[22] Gao Z K, Li T and Li Z H 2020 *Sci. China Phys. Mech. Astron.* **63** 120311
[23] Zad H A 2016 *Chin. Phys. Lett.* **33** 090302
[24] Li T, Wang Z K and Xia K Y 2020 *Opt. Express* **28** 1316
[25] Zhang W and Han Z F 2019 *Acta Phys. Sin.* **68** 070301 (in Chinese)
[26] Luo J W, Wu D W, Li X, Zhu H N and Wei T L 2019 *Acta Phys. Sin.* **68** 064204 (in Chinese)
[27] Briegel H J, Dür W, Cirac J I and Zoller P 1998 *Phys. Rev. Lett.* **81** 5932
[28] Li T, Yang G J and Deng F G 2016 *Phys. Rev. A* **93** 012302
[29] Li Y, Ye X J and Chen J L 2016 *Chin. Phys. Lett.* **33** 080301
[30] Kalb N, Reiserer A A, Humphreys P C, Bakermans J J W, Kamerling S J, Nickerson N H, Benjamin S C, Twitchen D J, Markham M and Hanson R 2017 *Science* **356** 928
[31] Wang G Y and Long G L 2019 *Sci. China Phys. Mech. Astron.* **63** 220311
[32] Wang G Y, Ai Q, Deng F G and Ren B C 2020 *Opt. Express* **13** 18693
[33] Bennett C H, Brassard G, Popescu S, Schumacher B, Smolin J A and Wootters W K 1996 *Phys. Rev. Lett.* **76** 722
[34] Deutsch D, Ekert A, Jozsa R, Macchiavello C, Popescu S and Sanpera A 1996 *Phys. Rev. Lett.* **77** 2818
[35] Pan J W, Simon C, Brukner Č and Zeilinger A 2001 *Nature* **410** 1067
[36] Sheng Y B, Deng F G and Zhou H Y 2008 *Phys. Rev. A* **77** 059902
[37] Zhou L, Zhong W and Sheng Y B 2020 *Opt. Express* **28** 2291
[38] Hu X M, Huang C X, Sheng Y B, Zhou L, Liu B H, Guo Y, Zhang C, Xing W B, Huang Y F, Li C F and Guo G C 2021 *Phys. Rev. Lett.* **126** 010503
[39] Riera S F, Sekatski P, Pirker A and Dür W 2021 *Phys. Rev. Lett.* **127** 040502
[40] Ecker S, Sohr P, Bulla L, Huber M, Bohmann M and Ursin R 2021 *Phys. Rev. Lett.* **127** 040506
[41] Sheng Y B and Deng F G 2010 *Phys. Rev. A* **81** 032307
[42] Sheng Y B and Deng F G 2010 *Phys. Rev. A* **82** 044305
[43] Ren B C and Deng F G 2013 *Laser Phys. Lett.* **10** 115201
[44] Ren B C, Du F F and Deng F G 2014 *Phys. Rev. A* **90** 052309
[45] Wang G Y, Li T, Ai Q, Alsaedi A, Hayat T and Deng F G 2018 *Phys. Rev. Appl.* **10** 054058
[46] Du F F, Liu Y T, Shi Z R, Liang Y X, Tang J and Liu J 2019 *Opt. Express* **27** 27046
[47] Wang P, Yu C Q, Wang Z X, Yuan R Y, Du F F and Ren B C 2022 *Front. Phys.* **17** 31501
[48] Murao M, Plenio M B, Popescu S, Vedral V and Knight P L 1998 *Phys. Rev. A* **57** R4075
[49] Cheong Y W, Lee S W, Lee J and Lee H W 2007 *Phys. Rev. A* **76** 042314
[50] Sheng Y B, Deng F G, Zhao B K, Wang T J and Zhou H Y 2009 *Eur. Phys. J. D* **55** 235
[51] Deng F G 2011 *Phys. Rev. A* **84** 052312
[52] Sheng Y B, Deng F G and Zhou H Y 2009 *Phys. Rev. A* **373** 1823
[53] Reithmaier J P, Sek G, Löffler A, Hofmann C, Kuhn S, Reitzenstein S, Keldysh L V, Kulakovskii V D, Reinecke T L and Forchel A 2004 *Nature* **432** 197
[54] Veldhorst M, Hwang J C C, Yang C H, Leenstra A W, de Ronde B, Dehollain J P, Muhonen J T, Hudson F E, Itoh K M, Morello A and Dzurak A S 2014 *Nat. Nanotechnol.* **9** 981
[55] Pursley B C, Carter S G, Yakes M K, Bracker A S and Gammon D 2018 *Nat. Commun.* **9** 115
[56] Berezovsky J, Mikkelsen M H, Stoltz N G, Coldren L A and Awschalom D D 2008 *Science* **320** 349
[57] Abe E, Wu H, Ardavan A and Morton J J L 2011 *Appl. Phys. Lett.* **98** 251108
[58] Lagoudakis K G, Fischer K, Sarmiento T, Majumdar A, Rundquist A, Lu J, Bajcsy M and Vučković J 2013 *New J. Phys.* **15** 113056
[59] Hu C Y, Munro W J, O'Brien J L and Rarity J G 2009 *Phys. Rev. B* **80** 205326
[60] Wang C, Zhang Y and Jin G S 2011 *Phys. Rev. A* **84** 032307
[61] Hu C Y, Young A, O'Brien J L, Munro W J and Rarity J G 2008 *Phys. Rev. B* **78** 085307
[62] An J H, Feng M and Oh C H 2009 *Phys. Rev. A* **79** 032303
[63] Wang T J, Song S Y and Long G L 2012 *Phys. Rev. A* **85** 062311
[64] Li T and Deng F G 2016 *Phys. Rev. A* **94** 062310
[65] Wei H R, Zheng Y B, Hua M and Xu G F 2020 *Appl. Phys. Express* **13** 082007
[66] Han Y H, Cao C, Fan L and Zhang R 2021 *Opt. Express* **29** 20045
[67] Somaschi N, Giesz V, De Santis L, Loredo J C, Almeida M P, Hornecker G, Portalupi S L, Grange T, Antón C, Demory J, Gómez C, Sagnes I, Lanzillotti-Kimura N D, Lemaître A, Auffeves A, White A G, Lanco L and Senellart P 2016 *Nat. Photon.* **10** 340